The Composition and Structure of Pd−Au Surfaces

C.-W. Yi, K. Luo, T. Wei, and D. W. Goodman*

Department of Chemistry, Texas A&M University, P.O. Box 30012, College Station, Texas 77842-3012

Received: June 28, 2005; In Final Form: August 9, 2005

Pd, Au, and Pd−Au mixtures were deposited via physical vapor deposition onto a Mo(110) substrate, and the surface concentration and morphology of the Pd−Au mixtures were determined by low-energy ion scattering spectroscopy (LEISS), infrared absorption spectroscopy (IRAS), temperature-programmed desorption (TPD), and X-ray photoelectron spectroscopy (XPS). Pd−Au mixtures form a stable alloy between 700 and 1000 K with substantial enrichment in Au compared to the bulk composition. Annealing a 1:1 Pd−Au mixture at 800 K leads to the formation of a surface alloy with a composition $Au_{0.8}Pd_{0.2}$ where Pd is predominantly surrounded by Au. The surface concentration of this isolated Pd site can be systematically controlled by altering the bulk Pd−Au alloy concentration.

Introduction

Bimetallic catalysts have attracted considerable attention because their properties often differ markedly from either of the constituent metals, with the mixtures frequently exhibiting enhanced catalytic stabilities, activities, or selectivities.[1] Research on alloy catalysts intensified in the late 1940s with the goal of establishing a direct link between electronic and catalytic properties;[2] however, little progress was made because of the technical difficulties encountered in the preparation and characterization of alloy surfaces. In the 1960s and 1970s, the development of bimetallic catalysts for hydrocarbon reforming in the petrochemical industry led to a renewed interest in catalysis by mixed metals.[3] Subsequent research provided the basis for the concepts of "ensemble" and "ligand" effects, widely used to describe the origin of the enhanced activity or selectivity of bimetallic catalysts.

The term "ensemble effects" has been used to describe a finite number of atoms in a particular geometric orientation that are required for facilitating a particular catalytic process. The addition of a second metal may block certain sites, effectively breaking up these ensembles and suppressing the reaction pathway promoted by that ensemble. This can substantially influence not only the selectivity of a reaction but also the activity of the catalyst if the formation of an inhibiting species or an important intermediate is reduced or eliminated.[4,5]

The term "ligand effects" refers to electronic modifications resulting from the addition of one metal to a second metal leading to the formation of heteronuclear metal−metal bonds involving either charge transfer between the metals or to orbital rehybridization of one or both of the metals. These changes lead to altered properties of the mixed-metal system including the catalytic activity.[4,5]

Palladium−gold (Pd−Au) alloys are frequently used as catalysts, for example, CO oxidation, synthesis of vinyl acetate monomer, hydrodechlorination of CCl_2F_2, hydrogenation of hydrocarbon, cyclotrimerization of acetylene, and so forth.[6−9] Pd is an excellent catalyst for many catalytic reactions, whereas Au alone is regarded as a poor catalyst. Recently, it has been shown that the activity and selectivity of Pd catalysts can be significantly enhanced by the addition of Au, and therefore Pd−Au alloy catalysts[10−12] and Pd−Au surfaces have been the subject of several investigations.[6−10,12−16] Pd and Au are completely miscible as a solid solution. Since there is only a 4% lattice mismatch between Pd(111) and Au(111),[17] flat, pseudomorphic overlayers of Pd on Au(111) and Au on Pd(111) can be prepared. Shen et al.[18,19] carried out studies of the growth of Pd overlayers on Au(111) and confirmed layer-by-layer growth at room temperature using Auger electron spectroscopy (AES). Maroun et al.,[20] using scanning tunneling microscopy (STM), also reported that Pd grown on Au(111) assumes a hexagonal structure with a lattice spacing equal to that of Au(111).

Surface composition is a key to understanding the role of alloying in mixed-metal catalysts. Several studies have shown that the surface of a Pd−Au alloy differs from the corresponding bulk concentration[13−16] with the differences generally attributed to differences in the surface free energies of Pd and Au. The results of these studies vary, ranging from a relative small Au enrichment using the Au (71 eV) and Pd (330 eV) Auger transitions to analyze the surface composition[13,16] to a significant enrichment of the surface in Au[14,15] using AES and low-energy ion scattering spectroscopy (LEISS). The marked differences between these studies[13−16] may be due to differences in the alloy preparation procedures. LEISS detects only the topmost surface layer and therefore is the preferred technique for assessing the outermost surface composition.

To facilitate the preparation of well-characterized mixed-metal compositions, a Mo(110) surface was used to support multilayers of Au and Pd deposited by physical vapor deposition. Considerable work has addressed the details of Au/Mo(110) and Pd/Mo(110). Park et al.[21] reported that a few monolayers of Pd on Mo(110) assume a distorted ⟨111⟩ structure; however, thicker films form a nearly perfect hexagonal Pd(111) bulk structure at room temperature.[21] AES and low-energy electron diffraction (LEED) studies of the growth of Au on Mo(110)[22,23] indicate a layer-by-layer growth with the first few overlayers growing pseudomorphic with respect to the substrate, eventually yielding a Au(111)-like surface structure. Mixtures of Pd and Au on Mo(110), on the other hand, have received only limited attention.[23]

* To whom correspondence should be addressed. E-mail: goodman@mail.chem.tamu.edu.

10.1021/jp053515r CCC: $30.25 © 2005 American Chemical Society
Published on Web 09/10/2005

In the present work, a combination of X-ray photoelectron spectroscopy (XPS) and LEISS were used to investigate the surface concentration, the extent of alloying, and the electronic properties of Pd−Au bimetallic films. Both infrared reflection absorption spectroscopy (IRAS) and temperature-programmed desorption (TPD) using CO as a probe molecule were used to elucidate the surface structure, the Pd−Au surface ensembles, and the corresponding variation in chemical properties. This study demonstrates a facile method for studying the surface versus bulk composition of mixed-metal phases using mutilayer metal films on a refractory metal substrate.

Experimental Section

The experiments were carried out in two ultrahigh vacuum chambers. The first chamber was equipped with XPS, LEISS, LEED, and TPD with a base operating pressure of 2×10^{-10} Torr. The XPS and LEISS spectra were collected using a concentric hemispherical analyzer (PHI, SCA 10-360). The second chamber was equipped with IRAS, AES, and TPD, with a base pressure of 2×10^{-10} Torr. The Mo(110) single crystal was mounted on a transferable probe capable of liquid nitrogen cooling to 85 K and resistive heating to 1600 K. In addition, the sample could be heated to 2400 K using an electron beam assembly. The sample temperature was monitored with a W-5% Re/W-26% Re (type C) thermocouple which was spot-welded to the back of the Mo(110) single crystal.

The sample was cleaned by oxidation and electron beam heating cycles and the surface cleanliness was confirmed by XPS, LEISS, and LEED. Au and Pd were deposited via physical vapor deposition using a resistively heated W filament wrapped with a high-purity wire of the corresponding metal. The metal dosers were thoroughly degassed and the dosing rates were calibrated by LEISS and TPD. The Mg Kα XPS spectra of the deposited overlayers were calibrated with respect to the substrate Mo $3d_{5/2}$ transition at 227.7 eV. LEISS was performed using He^+ ions at 1.09 keV and an ion beam scattering angle of ∼55° with respect to the surface normal. The beam was rastered (5 mm × 5 mm) to minimize the ion beam damage. The rate of the sputtering depletion during LEISS was determined to be negligible for the relatively low beam energy employed. The IR spectra were acquired using 4 cm^{-1} resolution and 512 scans in the single reflection mode at an incident angle of 85° with respect to the surface normal. In addition, the sample was heated at the desired temperature for 20 min and then was allowed to cool to room temperature before the XPS and LEISS were acquired.

Results and Discussion

XPS and LEISS. To investigate alloy formation, the electronic properties, and the surface concentration of the Pd−Au films, XPS and LEISS measurements were performed. For Pd, the less intense Pd $3d_{3/2}$ feature was monitored because of the overlap of the Pd $3d_{5/2}$ and the Au $4d_{5/2}$ peak. Figure 1 shows Au $4f_{7/2}$ and Pd $3d_{3/2}$ core-level binding energies as a function of annealing temperature for 5 ML Pd/5 ML Au/Mo(110) (Au deposited first) and 5 ML Au/5 ML Pd/Mo(110) films (Pd deposited first). For 5 ML Pd deposited on 5 ML Au/Mo(110), the XPS peak position of the Au $4f_{7/2}$ is 83.7 eV at 300 K, gradually shifting toward lower binding energies as the annealing temperature is increased to 600 K. Between 600 and 800 K, the Au $4f_{7/2}$ peak position is steady at 83.3 eV with a slight shift to 83.4 eV upon annealing to 1100 K. At 300 K, the XPS feature of Pd $3d_{3/2}$ is centered at 340.3 eV, gradually shifting to 340 eV at 700 K, then shifting back to 340.7 eV at 1200 K.

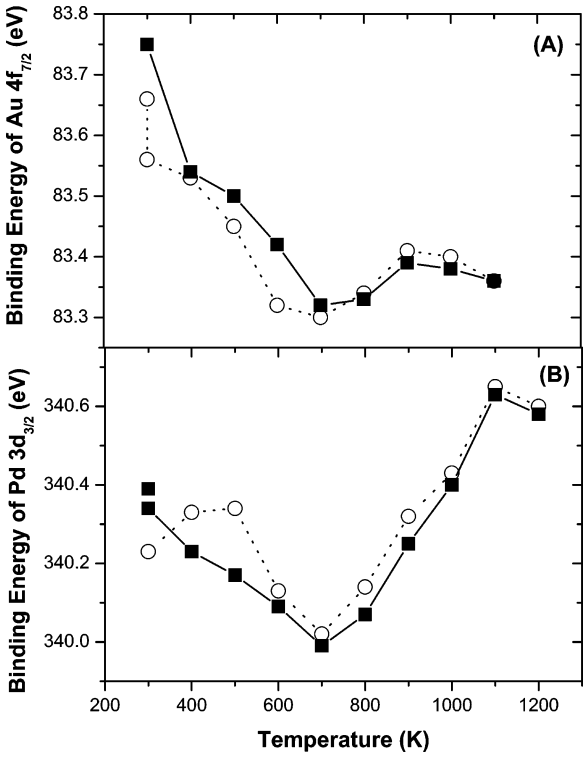

Figure 1. Core-level binding energy from XPS spectra of Au $4f_{7/2}$ (A) and Pd $3d_{3/2}$ (B) of 5 ML Pd/5ML Au/Mo(110) (○) and 5 ML Au/5ML Pd/Mo(110) (■) with respect to annealing temperature

Upon annealing to 800 K, the Au $4f_{7/2}$ and Pd $3d_{3/2}$ peak positions shift to lower binding energies by ∼0.45 eV and ∼0.15 eV, respectively, relative to bulk Au and Pd. Previously, Lee and co-workers[24] reported that the Pd $3d_{3/2}$ and the Au $4f_{7/2}$ core levels shift to lower binding energies upon alloying, and results are in excellent agreement with the core level shifts of Au $4f_{7/2}$ and Pd $3d_{3/2}$ seen here. These authors also assert that the core-level binding energy shifts conform to a charge compensation model and propose that Au gains sp-type electrons and loses d-electrons whereas Pd loses sp-electrons and gains d-electrons.[24] In any case, the core-level binding energy shifts observed here clearly show that alloy formation indeed occurs.

With a further increase in the annealing temperature, the core level of Pd $3d_{3/2}$ shifts to higher binding energy because of desorption of Au. The film thickness of Au−Pd alloy was monitored by attenuation of the Mo $3d_{5/2}$ feature. The thickness of the alloy film begins to decrease as the annealing temperature reaches 1000 K and is significantly reduced at 1100 K. Our TPD results (not shown) indicate that Au desorbs initially followed by Pd. Therefore, at annealing temperatures higher than 1000 K, the film thickness attenuates because of desorption of Au, and the binding energy of Pd $3d_{3/2}$ shifts to higher binding energy because of the strong interaction between Pd overlayers and the Mo substrate.[25]

LEISS was used to determine the surface composition of the Pd−Au alloy surfaces. Figure 2 shows the LEISS spectra of 5 ML Pd/5 ML Au/Mo(110) as a function of annealing temperature. Following deposition of 5 ML Au onto Mo(110) at 300 K, the Au LEISS feature appears at 1.03 keV whereas no Mo feature is observed at 0.94 keV. After Pd deposition onto 5 ML Au/Mo(110), the Pd LEISS feature appears at 0.97 keV, whereas the Au feature is significantly reduced. Because of the Pd−Au interdiffusion even at room temperature,[26] a Au LEISS feature was still apparent after deposition of 5 ML Pd. Upon annealing to 600 K, the Pd peak intensity gradually decreases with a

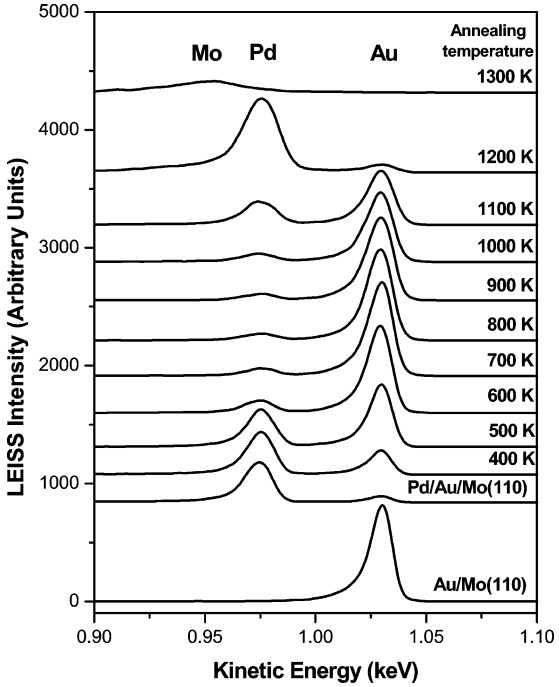

Figure 2. LEISS spectra of 5 ML Pd/5 ML Au/Mo(110) as a function of annealing temperature. LEISS spectra were collected at 300 K after the sample was annealed to the specified temperature.

corresponding increase in the Au peak intensity. At elevated annealing temperatures, Au−Pd interdiffusion is clearly apparent in the series of LEISS spectra of Figure 2. With further annealing up to 1000 K, the Au and Pd LEISS peak intensities change very little. Finally, the Au and Pd LEISS features disappear at 1200 and 1300 K, respectively, because of desorption of Au and Pd, with a concomitant appearance of Mo scattering features which appear at 0.94 keV following an anneal at 1300 K. Following an anneal at 1200 K, only trace amounts of Au are evident by XPS. Similar to the present work, Shih et al.[23] report alloying of Pd and Au at room temperature with the disappearance of the Pd Auger signal following an anneal as a result of Pd diffusion into Au. The Auger signals of Au significantly decrease and those of Mo and Pd reappear when a 1 ML Pd/multilayer Au/Mo(110) surface is heated to approximately 1150 K.[23]

On the basis of the results of Figure 2, the surface concentrations of each constituent of the 5 ML Pd−5 ML Au mixtures were calculated using eq 1.[27] For a Au−Pd alloy, the surface concentration of Au is given by

$$c_{\mathrm{Au}} = \frac{I_{\mathrm{Au}}}{I_{\mathrm{Au}} + f_{\mathrm{Au/Pd}} \cdot I_{\mathrm{Pd}}} \qquad (1)$$

where $f_{\mathrm{Au/Pd}}$ is the ratio of the scattering intensity for 10 ML Au and 10 ML Pd, and I_{Au} and I_{Pd} are the scattering intensity from Au and Pd from the alloy surfaces, respectively.[27,28] Figure 3 shows the surface concentrations of Pd and Au as a function of annealing temperature. For a 5 ML Pd/5 ML Au surface (open circle and dashed line), the surface concentration of Au gradually increases from 4 to 80% with increasing anneal temperature up to 700 K. Between 700 and 1000 K, the surface composition of Pd and Au, $Au_{0.8}Pd_{0.2}$, remains constant. These results are consistent with considerations of the surface free energy, that is, the surface free energy of Pd (2.043 J/ m^2)[29] is higher than that of Au (1.626 J/m^2).[30] Hence, to minimize the surface free energy, Au preferentially decorates the surface. Above 1000

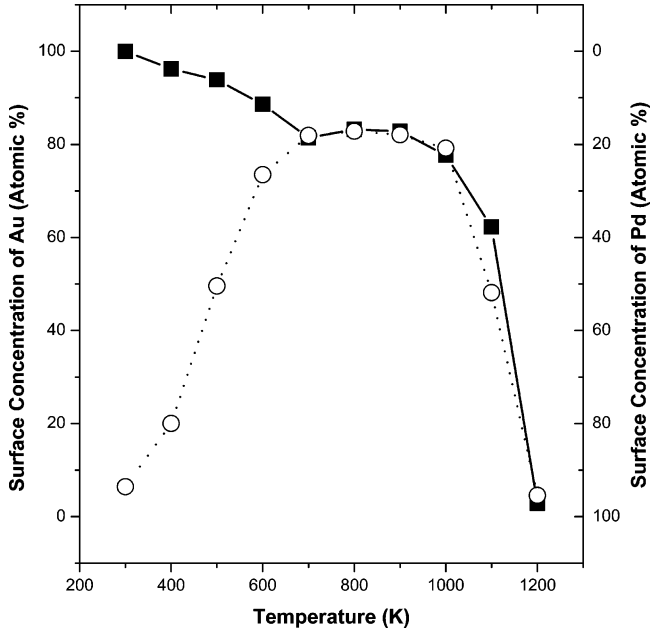

Figure 3. Surface concentration of Au and Pd of 5 ML Pd/5 ML Au/Mo(110) (○) and 5 ML Au/5 ML Pd/Mo(110) (■) as a function of annealing temperature. The sample was annealed at each temperature for 20 min.

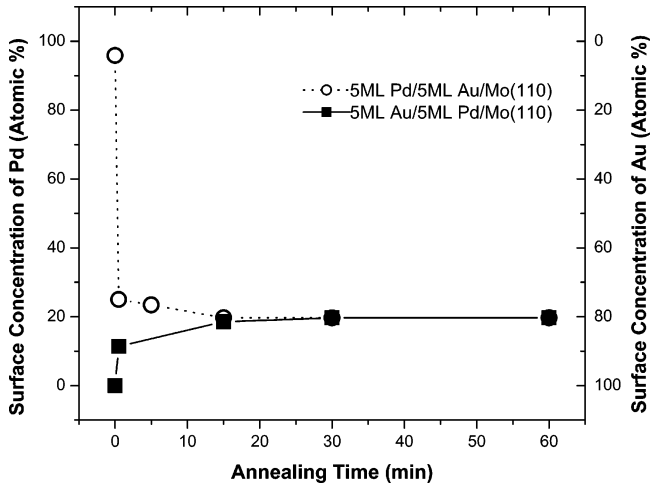

Figure 4. Surface concentration of 5 ML Pd/5 ML Au/Mo(110) and 5 ML Au/5 ML Pd/Mo(110) measured by LEISS as a function of annealing time at 800 K.

K, the Au surface concentration abruptly decreases because of Au desorption and Pd becomes dominated on the surface. LEISS experiments of the inverted system, 5 ML Au/5 ML Pd/Mo(110) (filled square), were also carried out, and the surface concentrations of Pd and Au for each system were similarly calculated as above. For 5 ML Au/5 ML Pd/Mo(110), the Pd surface concentration gradually increases from 0 to 20% up to 700 K, where an alloy surface, $Au_{0.8}Pd_{0.2}$, forms and remains stable up to 1000 K. At higher annealing temperatures, the Pd surface concentration increases significantly because of Au desorption. Therefore, independent of the order of deposition, 5 ML Pd−5 ML Au mixtures form a stable alloy between 700 and 1000 K, with a surface consisting of ∼20% Pd and ∼80% Au.

Figure 4 shows the surface concentrations of Au and Pd for 5 ML Pd−5 ML Au on Mo(110) as a function of annealing time at 800 K. After depositing 5 ML Pd onto 5 ML Au/Mo(110) at room temperature, the Au and Pd surface compositions

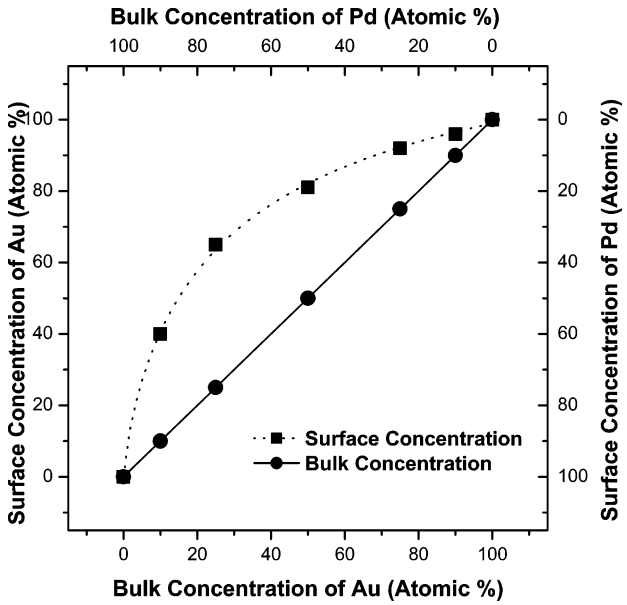

Figure 5. Surface concentration of various Pd−Au alloys on Mo(110) measured by LEISS compared to the corresponding bulk concentration. The sample was annealed at 800 K for 20 min.

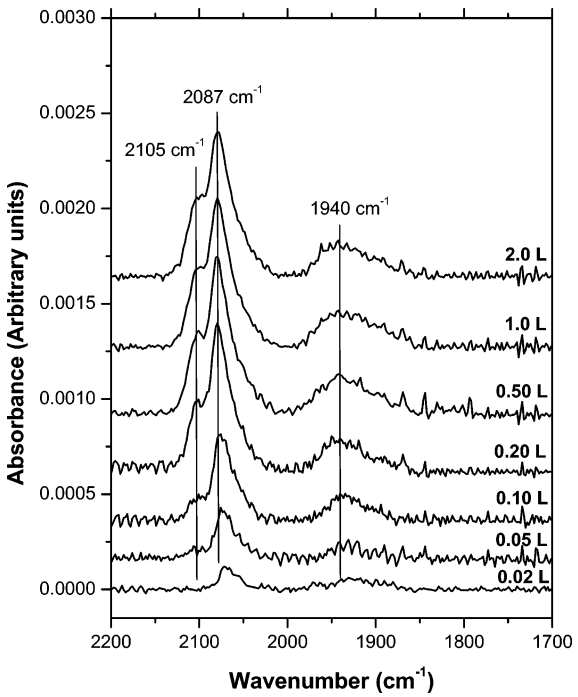

Figure 6. IRAS of CO on 5 ML Pd/5 ML Au/Mo(110), annealed at 600 K for 20 min, as a function of CO exposure.

are 4 and 96 atomic %, respectively, as shown in Figure 3. Following a flash to 800 K, the surface concentration of Au increases to 74 atomic % whereas Pd is reduced to 26 atomic % within 1 min; subsequently, the concentration of Au gradually increases with anneal time. The initial increase in Au and decrease in Pd surface concentration suggests the rapid Pd−Au interdiffusion. After a 15-min anneal at 800 K, the surface concentration of Au and Pd changes to 82 and 18 atomic %, respectively, and the surface concentration remains constant with further annealing. In the inverted system, 5 ML Au/5 ML Pd/Mo(110), the surface is 89% Au and 11% Pd after a flash to 800 K; the surface composition is constant at 82% of Au and 18% of Pd after a 15-min anneal. The surface concentrations of Au and Pd for both systems converge after a 15-min anneal, in excellent agreement with the results of Figure 2, and are consistent with the formation of a stable surface alloy formation.

To further investigate the surface concentration of Pd−Au, LEISS experiments were carried out on different ratios of Pd−Au at a constant total thickness of 10 ML. In Figure 5, the surface (filled circle and dashed line) versus bulk concentration (filled square and straight line) phase diagram is plotted as a function of the Pd/Au ratio. The Pd−Au mixtures were annealed at 800 K for 20 min, and the surface composition was determined by LEISS at 300 K. The results show that the surface composition is quite different from the bulk. The surface concentrations of Au range from 40% to 96% while the Au bulk concentration varies from 10% to 90%. For a 1:1 Pd−Au bulk ratio, the surface consists of 82% Au atoms. For a 1:3 Pd−Au mixture, the surface content is 93.5% Au, and for a 3:1 Pd−Au mixture, 65% Au at 800 K. Swartzfager et al.[15] carried out $^{20}Ne^{+}$ LEISS experiments to investigate the surface concentration of Pd−Au alloys, prepared by melting high-purity Au and Pd in a vacuum induction furnace. These authors observed preferential Au segregation following an anneal and reported the surface compositions to greatly differ from the bulk. For example, a 2:3 and 3:2 Pd−Au mixture exhibited 85 and 70% Au, respectively, at the surface. The surface compositions found in the present study are consistent with this previous study. This correlation confirms the efficacy of the thin-film methodology used in the current studies. These data also clearly show that the surface composition can be systematically controlled by altering the bulk Pd−Au alloy concentration.

IRAS and TPD. IRAS was carried out with CO as a probe molecule to determine the structure of Pd−Au surface ensembles. Figure 6 shows IRAS spectra as a function of the CO exposure at 90 K onto a 5 ML Pd/5 ML Au surface annealed at 600 K for 20 min. Following a relatively low exposure of CO (<0.10 L), IRAS shows mainly two stretching features at 2087 and 1940 cm^{-1}, frequencies typical of linearly and bridged-bound CO on metal surfaces, respectively. CO on Pd(111) shows vibrational frequencies characteristic of the particular bonding sites on a Pd surface: typically 2110−2080 cm^{-1} for linearly bound CO, 1965−1900 cm^{-1} for 2-fold bridging CO, and 1900−1800 cm^{-1} for 3-fold bound CO species.[31,32] Koel and co-workers carried out a high-resolution electron energy loss spectroscopy (HREELS) study of CO on 1 ML Pd deposited on Au(111) at 125 K and reported two energy losses at 1910 and 2090 cm^{-1}, assigned to CO on 2-fold bridging and atop sites of Pd, respectively.[26] Our results are consistent with these CO vibrational assignments. With further CO exposure (≥0.20 L), a new feature appears at 2105 cm^{-1} and saturates at 0.5 L CO dose. The feature at 2105 cm^{-1} is assigned to CO on a Au atop site since the vibrational frequency of CO on atop sites of Au fall within the range 2120−2100 cm^{-1}, depending on the surface structure of Au and the coverage of CO.[33] Behm and co-workers also assigned the 263 meV (2119 cm^{-1}) energy loss feature to a weakly adsorbed linearly bound CO species on Au of Au/Pd(111) in their HREELS study.[34,35]

Figure 7A shows IRAS spectra acquired at 90 K for CO adsorbed on a 5 ML Pd/5 ML Au surface annealed at 800 K for 20 min. A feature at 2087 cm^{-1} appears within the low coverage CO regime (<0.10 L). With additional CO exposure, a second feature emerges at 2112 cm^{-1} and is assigned to CO on atop sites of Au; both features saturate at 0.50 L CO exposure. The thermal behavior of CO on this alloy surface is shown in Figure 7B. The feature at 2112 cm^{-1} is attenuated with increasing surface temperature and completely disappears above 125 K. Above 125 K, IRAS shows only one feature at

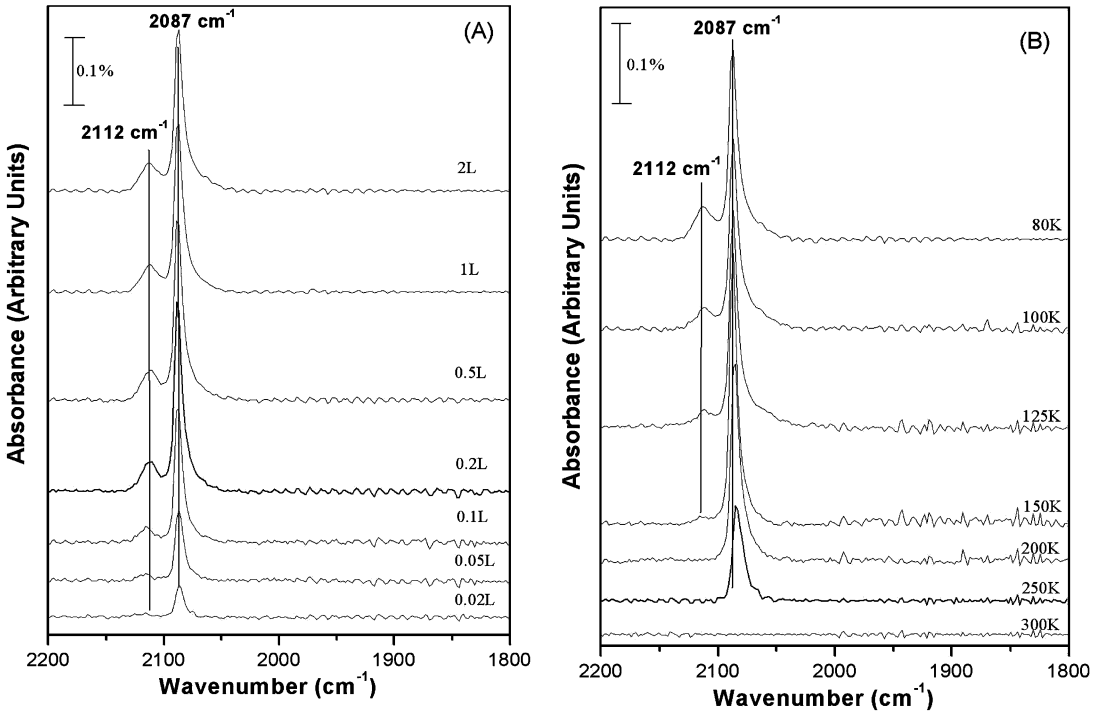

Figure 7. IRAS of CO adsorbed on 5 ML Pd/5 ML Au/Mo(110) annealed at 800 K for 20 min: (A) CO IRAS as a function of CO exposure; (B) CO IRAS with respect to the surface temperature.

2087 cm^{-1}, a feature that disappears at 300 K. Multifold CO vibrational features were not observed on this surface, indicating that CO adsorbs only on Pd atop sites and that Pd is isolated as a singleton species. In excellent agreement with our results, Behm and co-workers[34,35] performed HREELS of CO on Au/Pd(111). Several loss features at 263, 258, and 237−240 meV (2119, 2081, and 1912−1936 cm^{-1}) of CO adsorbed on Au/Pd(111) were observed. As mentioned above, the 263 meV loss feature was assigned to CO adsorbed on Au sites. The loss features at 258 and 237−240 meV were assigned to CO species adsorbed to Pd atoms coordinated to Au and to CO adsorbed on small Pd patches, respectively. With a low-temperature anneal (450−600 K) of Au/Pd(111), the surface becomes Au-rich with pronounced CO stretching features appearing at 258 meV. As the annealing temperature is increased, the surface becomes Pd-rich. Above 700 K, the intensity of the 258 meV CO species reaches a maximum and then attenuates with further annealing. The 237−240 meV feature clearly dominates. From our LEISS analysis in Figure 4, the surface concentration of Pd is reduced by 18% upon annealing a 5 ML Pd/5 ML Au/Mo(110) surface at 800 K for 20 min whereas the alloy surface annealed at 600 K for 20 min has 27% surface Pd. Since the alloy surface becomes Au-rich surface with an increase in the anneal temperature, the density of larger surface Pd ensembles (e.g., Pd-dimer, Pd-trimer, Pd patches, etc.) is very low on this alloy surface because of the strong interdiffusion of Pd into Au. Therefore, the results suggest that the most probable surface ensemble is a Pd monomer decorated with Au atoms.

The combination of CO TPD and IRAS allows characterization of the available chemisorption sites and an estimation of their variation with surface concentration. Figure 8 shows a series of CO TPD from 5 ML Pd/5 ML Au alloy system, annealed at 800 K for 20 min and then exposed to CO at 90 K. From the LEISS analysis, the surface concentration of this surface is 18 and 82 atomic percent of Pd and Au, respectively. With a small amount of CO (<0.20 L), the main desorption feature appears at ∼300 K. With further CO exposure (0.50

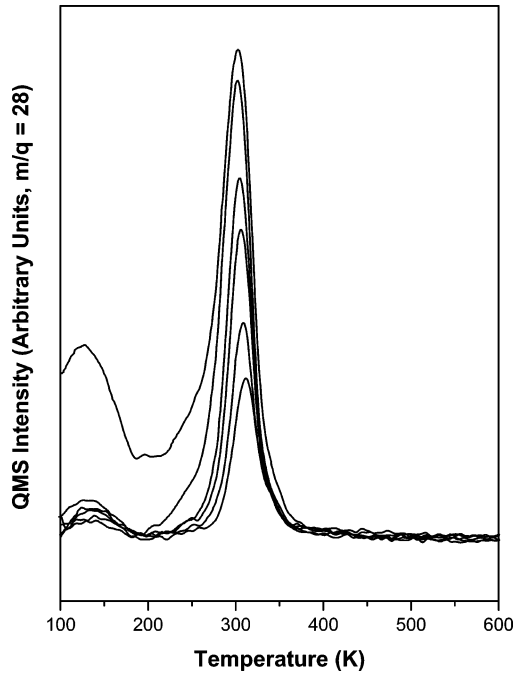

Figure 8. TPD of CO on 5 ML Pd/5 ML Au/Mo(110) annealed at 800 K for 20 min (0.01∼0.5 L of CO).

L), this desorption feature is saturated and shifts to 295 K, and a new feature appears at 125 K. These two desorption features at 125 and 295 K are assigned to CO desorption from Au and Pd atop sites, respectively. For Pd(111), the peak desorption temperature maximum for CO is ∼450 K[31] and is assigned to the desorption of multifold CO; our TPD results show no desorption feature of CO above 350 K. These TPD results clearly show that there are no multifold adsorption sites for CO and that CO occupies atop Pd and Au sites. These TPD results are consistent with our IRAS data (Figure 7B) which show no multifold CO vibrational feature. Previously, Baddeley et al.[36]

reported a 2100 cm^{-1} loss and a 300 K TPD feature, assigned to CO on Pd singleton sites, and a 1930 cm^{-1} feature and a 445 K TPD feature, associated with 3-fold sites for annealed Au/Pd(111). Therefore, we conclude that the 125 K TPD feature and the 2112 cm^{-1} IR peak can be reasonably assigned to linearly bound CO on Au sites and the 295 K peak and 2087 cm^{-1} feature to linearly bound CO on singleton Pd sites surrounded by six gold atoms.

Our IRAS and TPD data as a function of the surface alloy concentration measured by LEISS allow determination of the relationship between the surface ensemble structure and the surface composition. A 1:1 Pd−Au mixture annealed at 800 K has 18% Pd surface content and shows no multiply coordinated CO IR features (Figure 7A) whereas the alloy annealed at 600 K, consisting of 27% surface Pd, shows evidence of a feature corresponding to multiply coordinated CO at 1940 cm^{-1} (Figure 6). Similarly, Behm and co-workers[20] recently reported the formation of similar Pd ensembles in a Pd/Au(111) surface synthesized using electrochemical methods. On the basis of their STM and IR data, the prevalent ensemble for CO adsorption on Pd/Au(111) is a Pd-monomer. At low Pd compositions (7 or 15%), only CO IR features corresponding to linearly bound CO on Pd-monomers were observed. This linearly bound CO feature increases in intensity up to 22% surface Pd, where bridged-bound features emerge and increase in intensity with an increase in the Pd concentration.

Conclusions

The composition, electronic properties, and structure of Pd−Au alloy surfaces were determined by LEISS, XPS, IRAS, and TPD. Preferential surface segregation of Au in Pd−Au mixtures on Mo(110) was observed after an anneal. Au and Pd films on Mo(110) form stable surface alloys which have fixed surface compositions within the temperature range 700−1000 K. Upon annealing at 800 K, 1:1 Pd−Au alloy mixtures form a stable alloy with a composition of $Pd_{0.2}Au_{0.8}$, independent of the metal deposition sequence. The most prevalent surface ensemble is an isolated Pd surrounded by Au. From LEISS results for various Pd−Au mixtures on Mo(110), the surface versus bulk phase diagram shows significant enrichment of the surface in Au compared to the bulk. The surface concentration of isolated Pd monomers can be systematically controlled by altering the bulk Pd−Au alloy concentration on Mo(110).

Acknowledgment. We gratefully acknowledge the support of this work by the Department of Energy, Office of Basic Energy Sciences, Division of Chemical Sciences, and the Robert A. Welch Foundation.

References and Notes

(1) Nascimento, M. A. C. *Theoretical aspects of heterogeneous catalysis*; Kluwer Academic Publishers: Dordrecht, The Netherlands; 2001; Vol. 8.
(2) Schwab, G. M. *Discuss. Faraday Soc.* **1950**, *8*, 166.
(3) Sinfelt, J. H. *Acc. Chem. Res.* **1977**, *10*, 15.
(4) Sinfelt, J. H. *Bimetallic catalysts: discoveries, concepts, and applications*; Wiley: New York, 1983.
(5) Chen, M. S.; Kumar, D.; Yi, C. W.; Goodman, D. W. *Science* submitted.
(6) Baddeley, C. J.; Ormerod, R. M.; Stephenson, A. W.; Lambert, R. M. *J. Phys. Chem.* **1995**, *99*, 5146.
(7) Han, Y. F.; Kumar, D.; Goodman, D. W. *J. Catal.* **2005**, *230*, 353.
(8) Legawiec-Jarzyna, M.; Srebowata, A.; Karpinski, Z. *React. Kinet. Catal. Lett.* **2003**, *79*, 157.
(9) Venezia, A. M.; La Parola, V.; Pawelec, B.; Fierro, J. L. G. *Appl. Catal., A* **2004**, *264*, 43.
(10) Landon, P.; Collier, P. J.; Papworth, A. J.; Kiely, C. J.; Hutchings, G. J. *Chem. Commun.* **2002**, 2058.
(11) Massalski, T. B.; Okamoto, H.; Subramanian, P. R.; Kacprzak, L. *Binary alloy phase diagrams*; ASM International: Materials Park, OH, 1990.
(12) Sarkany, A.; Horvath, A.; Beck, A. *Appl. Catal., A* **2002**, *229*, 117.
(13) Hilaire, L.; Legare, P.; Holl, Y.; Maire, G. *Surf. Sci.* **1981**, *103*, 125.
(14) Jablonski, A.; Overbury, S. H.; Somorjai, G. A. *Surf. Sci.* **1977**, *65*, 578.
(15) Swartzfager, D. G.; Ziemecki, S. B.; Kelley, M. J. *J. Vac. Sci. Technol.* **1981**, *19*, 185.
(16) Wood, B. J.; Wise, H. *Surf. Sci.* **1975**, *52*, 151.
(17) Koel, B. E.; Sellidj, A.; Paffett, M. T. *Phys. Rev. B* **1992**, *46*, 7846.
(18) Shen, X. Y.; Frankel, D. J.; Hermanson, J. C.; Lapeyre, G. J.; Smith, R. J. *Phys. Rev. B* **1985**, *32*, 2120.
(19) Shen, X. Y.; Frankel, D. J.; Lapeyre, G. J.; Smith, R. J. *Phys. Rev. B* **1986**, *33*, 5372.
(20) Maroun, F.; Ozanam, F.; Magnussen, O. M.; Behm, R. J. *Science* **2001**, *293*, 1811.
(21) Park, C.; Bauer, E.; Poppa, H. *Surf. Sci.* **1985**, *154*, 371.
(22) Gillet, E.; Gruzza, B. *Surf. Sci.* **1980**, *97*, 553.
(23) Shih, H. D.; Bauer, E.; Poppa, H. *Thin Solid Films* **1982**, *88*, L21.
(24) Lee, Y. S.; Jeon, Y.; Chung, Y. D.; Lim, K. Y.; Whang, C. N.; Oh, S. J. *J. Korean Phys. Soc.* **2000**, *37*, 451.
(25) Rodriguez, J. A.; Campbell, R. A.; Goodman, D. W. *J. Phys. Chem.* **1991**, *95*, 5716.
(26) Sellidj, A.; Koel, B. E. *Phys. Rev. B* **1994**, *49*, 8367.
(27) Niehus, H.; Heiland, W.; Taglauer, E. *Surf. Sci. Rep.* **1993**, *17*, 213.
(28) Varga, P.; Hetzendorf, G. *Surf. Sci.* **1985**, *162*, 544.
(29) Mezey, L. Z.; Giber, J. *Jpn. J. Appl. Phys.* **1982**, *21*, 1569.
(30) Anton, R.; Eggers, H.; Veletas, J. *Thin Solid Films* **1993**, *226*, 39.
(31) Guo, X. C.; Yates, J. T. *J. Chem. Phys.* **1989**, *90*, 6761.
(32) Ozensoy, E.; Goodman, D. W. *Phys. Chem. Chem. Phys.* **2004**, *6*, 3765.
(33) Meier, D. C.; Goodman, D. W. *J. Am. Chem. Soc.* **2004**, *126*, 1892.
(34) Gleich, B.; Ruff, M.; Behm, R. J. *Surf. Sci.* **1997**, *386*, 48.
(35) Ruff, M.; Frey, S.; Gleich, B.; Behm, R. J. *Appl. Phys. A* **1998**, *66*, S513.
(36) Baddeley, C. J.; Tikhov, M.; Hardacre, C.; Lomas, J. R.; Lambert, R. M. *J. Phys. Chem.* **1996**, *100*, 2189.